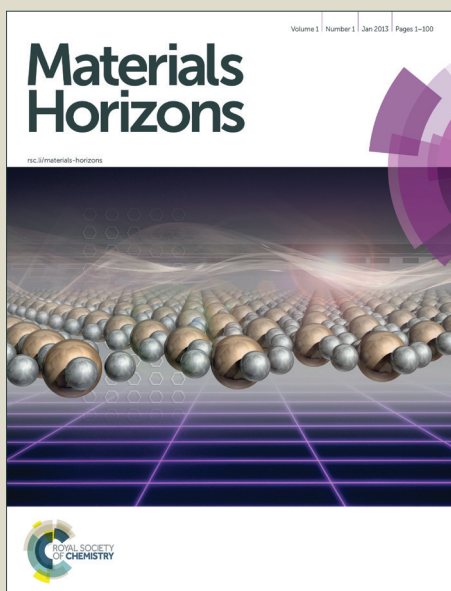


Materials Horizons

Accepted Manuscript



This is an *Accepted Manuscript*, which has been through the Royal Society of Chemistry peer review process and has been accepted for publication.

Accepted Manuscripts are published online shortly after acceptance, before technical editing, formatting and proof reading. Using this free service, authors can make their results available to the community, in citable form, before we publish the edited article. We will replace this *Accepted Manuscript* with the edited and formatted *Advance Article* as soon as it is available.

You can find more information about *Accepted Manuscripts* in the [Information for Authors](#).

Please note that technical editing may introduce minor changes to the text and/or graphics, which may alter content. The journal's standard [Terms & Conditions](#) and the [Ethical guidelines](#) still apply. In no event shall the Royal Society of Chemistry be held responsible for any errors or omissions in this *Accepted Manuscript* or any consequences arising from the use of any information it contains.

ARTICLE

Magic PAF-1 and Its Derivatives

Cuiying Pei,^a Teng Ben,^{b*} and Shilun Qiu^{a*}Cite this: DOI: 10.1039/x0xx00000x
Accepted 00th January 2012

DOI: 10.1039/x0xx00000x

www.rsc.org/

In materials design and preparative chemistry, it is imperative to understand the thought and logic behind synthesizing a particular kind of material. Computational modelling can help in this regard by not only optimizing the ideal materials but also by simulating their properties. Furthermore, the experimental result fills the gap that the complicated practical condition can't be covered by theoretical calculation. In this work, we focus on PAF-1 and its derivatives in order to analyse the correlations between the nature of the material (e.g. pore size, surface area, pore volume, functional groups, metal sites, interpenetrated frameworks) and properties such as gas sorption capacity, molecular recognition and separation.

Introduction

PAF-1 which linked the tetrahedron rigid building blocks with robust covalent bond was synthesized and reported in 2009.^[1] One year later, Cooper et al. succeeded in producing network 1^[2] with the same structure as PAF-1. In 2011, PAF-1 was resynthesized and renamed as PPN-6 by Zhou group^[3]. The most attractive feature of PAF-1 is that it successfully combines ultrahigh surface area ($S_{\text{BET}} = 5600 \text{ m}^2 \text{ g}^{-1}$) with high physicochemical stability. Hence, it can be used repeatedly for storage of hydrogen and methane as clean energy alternatives and also for capturing greenhouse gases like carbon dioxide under harsh conditions. In addition, the high physicochemical stability of PAF-1 makes it tolerant of modification conditions and facilitating formation of functionalized framework retains the structural advantage. This provides scope for modification of PAF-1 thereby extending its applications.

The modifications can be divided into three methods namely (1) pre-modification method where the basic monomer is decorated with hybrid atoms^[4,5] or heterocyclic units^[6,7], and linked by organic building blocks of different lengths^[6,7,8] or widths^[9,10,11]; (2) post-synthesis modification (PSM) method, which involves chemical functionalization of PAF-1 with functional groups^[3,12], metal atoms or ions^[13,14,15], (3) carbonization of PAF-1^[16,17]. (Fig. 1) Multiple modification

methods make possible the tuning of the pore size and the electric field density and distribution.

The study of PAF-1 also successfully demonstrates the idea of targeted synthesis. Conventionally, the hit and miss approach in synthetic chemistry not only exhausts the chemical resources but also cannot predict the characteristics of the obtained products. Theoretical studies can provide reliable calculations that can guide a design strategy and prevent chemists from aimless trials.

Specifically, PAF-1 was modelled by replacement of the C-C covalent bonds of diamond with rigid phenyl rings. Computational studies indicate that replacement of one phenyl ring yields a P1 structure which has lower surface area while replacement of three phenyl rings constructs a mesoporous P3 structure.^[1] In comparison, replacement of two phenyl rings makes a P2 structure showing surface area, density, and void framework at just the right level. As expected, empiric evaluation of the ultrahigh surface area ($S_{\text{BET}} = 5600 \text{ m}^2 \text{ g}^{-1}$)^[1] coincides well with the simulation ($S_{\text{BET}} = 5640 \text{ m}^2 \text{ g}^{-1}$)^[11].

The mechanism of formation of PAF-1 may explain the ordered crystal oligomer with *dia* topology formed at the beginning of the reaction. As condensation proceeds, defects are generated inevitably. Since the Yamamoto^[18] type Ullmann reaction^[19] is an irreversible process, the defects are not corrected by reassembly and, ultimately, expands further.



Cuiying Pei received her B. Sc. degree in chemistry from Harbin Normal University in 2008. Cooperation researched with the state key laboratory of inorganic synthesis and preparative chemistry, Jilin University and obtained her M. S. degree in 2011. After that, she became a Ph.D. student in the group of Prof. Shilun Qiu. Her research interests are the design and synthesis of novel porous organic frameworks for the applications in gas storage, separation and nanodevices.



Teng Ben received his PhD in 2002 from Jilin University on polymer science. After graduation, he joined the faculty at Jilin University, working with Prof. Zhongwen Wu as Lecturer. In 2005, he moved to Prof. Eiji Yashima group, at Nagoya University in Japan as a postdoctoral researcher. In 2008, he moved back to Jilin University as an Associate Professor and was promoted to Professor in 2010. His research interests include the fundamental understanding of host-guest interactions in nanoporous materials, gas storage and separation using porous organic frameworks.

Finally, a hybrid structure consisting of *dia* topology crystal and continuous random network (CRN) phase of SiO₂^[20] is obtained. Utilization of a rigid monomer effectively prevents single bond rotation which can block the structural rearrangement which could have caused the collapse of the porous structure.^[21] Calculation predicts a restricted pore size of PAF-1 which is too small for constituent monomer diffusion and a non-interpenetrated framework results.^[22] Derivatives with more void space will dispose to higher levels of interpenetration and minimize systematic energy.^[23] Hence PAF-1 exhibits high thermal stability in the range of the porous organic frameworks characterized by their ultrahigh stability, such as COF-102 (thermal stable beyond 450 °C)^[24] and ZIF-300, 301, 302, (stable to water and 450 °C dry air)^[25]. Besides, PAF-1 shows the narrow uniform pore size distribution. Its surface area is next only to MOF-210 ($S_{\text{BET}} = 6240 \text{ m}^2 \text{ g}^{-1}$)^[26], PPN-4 ($S_{\text{BET}} = 6461 \text{ m}^2 \text{ g}^{-1}$)^[27] and NU-110 ($S_{\text{BET}} = 7000 \text{ m}^2 \text{ g}^{-1}$)^[28]. Based on these favourable characteristics, derivatives constructed by tuning pore size, tailoring organic building blocks and modification of frameworks demonstrate improved properties and expand application areas. Herein, we summarize both the simulation and experimental studies on PAF-1^[1] and its derivatives (Fig. 2). We focus on the key structural factors that influence such remarkable properties. This work will provide valuable information for guiding the future work in material design and preparative chemistry.

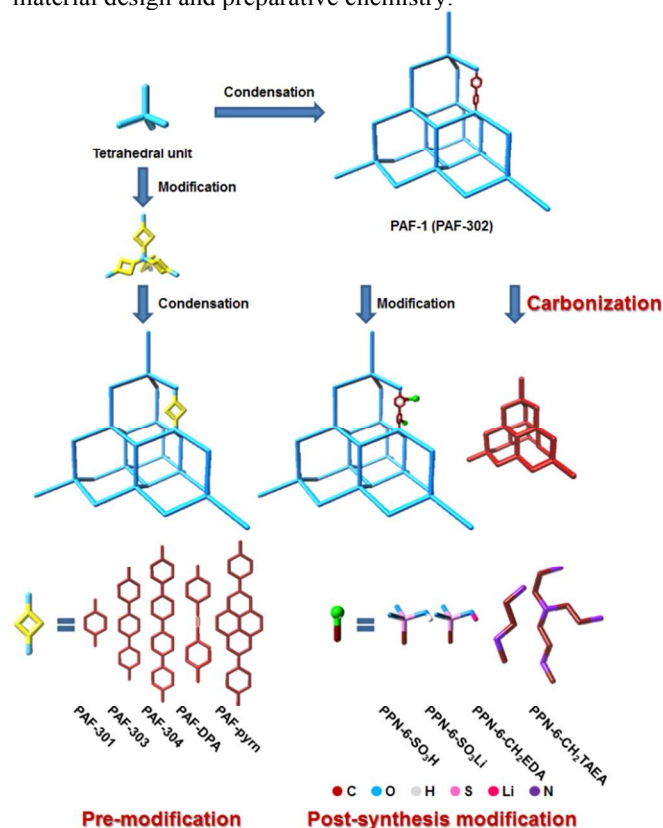


Figure 1. Strategy to construct and modify PAF-1 as well as several typical examples. In cyan stick constructs of *dia* topology frameworks, a yellow square stands for a functionalized link, a dark red stick represents a carbon unit and blue, grey, pink, magenta and purple represent oxygen, hydrogen, sulphur, lithium and nitrogen respectively.

Design principle

Tailoring pore size

The effect of pore size on molecule sorption and separation has been widely investigated. Presser et al. reported that pores smaller than 0.8 nm contributed the most to the CO₂ uptake at 1 bar, and the effect of 0.5 nm pores exhibited more uptake at 0.1 bar.^[29] For hydrogen storage, porous material with a pore size of two gas diameters is preferred.^[27,30] On the other hand, for molecule separation the material with pore size between the kinetic diameters of two different guest molecules can be directly used for separation. Even in cases where the pore size of material is larger than the kinetic diameters of molecules, the molecule with a dimension closer to the pore size will be retained while the other molecule can be exhausted. This has been confirmed by Grand Canonical Monte Carlo (GCMC) simulation results on diamondyne and PAF-302.^[31] Hence, design and synthesis of porous material with targeted pore size is one of the key strategies in this field. Generally, two effective methods to tune the pore size are: selection of organic building blocks with different lengths or structures versus functionalization of the framework.

The covalent bonds in the robust hydrocarbon scaffold PAF-1 contribute not only to the high physicochemical stability, but also to the low bulk density and high pore volume. Based on this topology, a series of porous organic materials has been designed by pore size tuning for different application requirements. PAF-301, PAF-302, PAF-303, PAF-304^[32,33] belong to the cubic space group P1. (Fig. 1) The difference is the number of phenyl rings between two neighbouring tetrahedral bonded carbon atoms. Without interpenetration, pore size of PAF-30X widens with the increase in phenyl ring linkages, to the extent that PAF-304 exhibits mesoporosity.^[32,33] GCMC simulation was chosen to evaluate the hydrogen, methane, and carbon dioxide storage as well as gas separation performance. It shows that PAF-304 possesses the highest gravimetric hydrogen uptake among the others due to the high pore size and pore volume. The value reaches 6.53 wt% at 298 K/100 bar. However, PAF-301 with the smallest pore of 5.2 Å shows not only the highest CO₂ uptake (275 mg g⁻¹ at 298 K/1 bar) at low pressure range, but also exhibits higher selectivity for the CO₂/H₂, CO₂/N₂, CO₂/CH₄, and CH₄/H₂ among PAF-30X.^[32,33]

Another strategy to tune the pore size is to construct PAFs with different widths and number of aromatic rings. Kuc et al. studied the mechanical and the hydrogen adsorption properties



Shilun Qiu received his Ph.D. in chemistry from Jilin University in 1988. He joined the University De Haute-Alsace, France, and Hokkaido University Sapporo, Japan, for postdoctoral research. In 1994, he was promoted to be a full professor in the Department of Chemistry, Jilin University. He won the Second Grade Award for the State Natural Science Award of China in 2008 and is a fellow of RSC. His recent research interests focus on the studies of molecular engineering, synthesis and catalysis of micro- and mesoporous materials, rational synthesis and hydrogen

storage of porous organic framework materials and host-guest chemistry, in particular, nano-composites in porous materials.

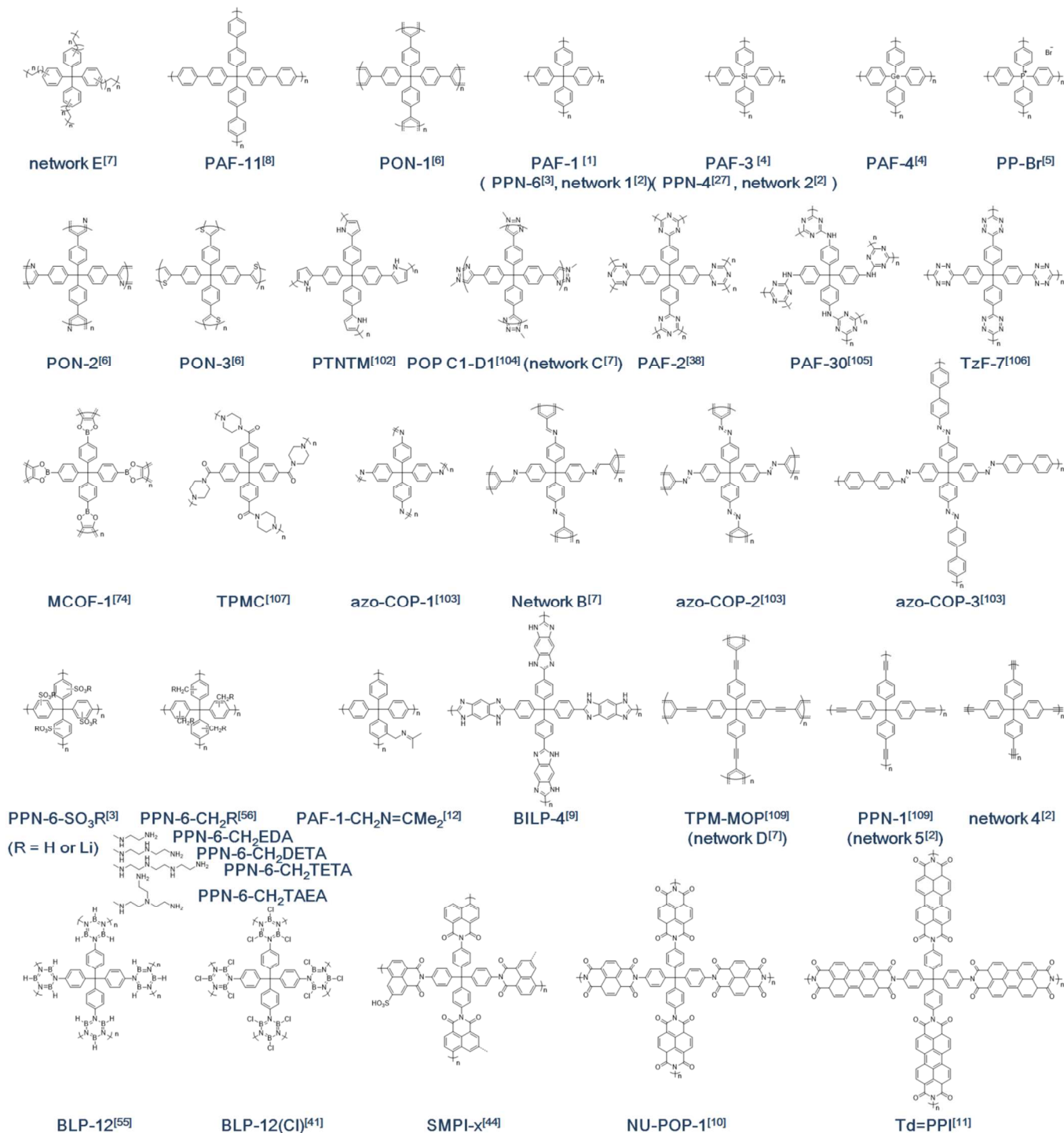


Figure 2. The structure summary of PAF-1 and its derivatives.

of these materials by density functional based tight-binding (DFTB) method and quantized liquid density functional theory (QLDFT).^[34-37] Exothermic formation energies of PAFs, calculated with regard for PAFs formed by saturated linkers and CH₄ molecule by dehydrogenation reaction, indicate strong coordinating linkers in *dia* topology. The mechanical stability decreases with increase in length of organic linkers; however, it strengthens with the expansion of width of the linker. Aromatic building blocks provide binding sites for hydrogen *via* London

dispersion forces. Long linkers expand the pore volume and decrease the mass density, which offer more space for hydrogen storage, and show significantly higher hydrogen gravimetric capacity. On the other hand, the wider linkers increase the surface area per volume and enhance the interaction between guest molecule and host framework.

It should be noted that large open skeletons are always accompanied by interpenetrative structures. The interpenetrated material has minimal entropy due to filling of void space

leading to repulsive forces which enhance the stability of framework.^[38] Although interpenetration both reduces pore size and pore volume and raises the bulk density, it creates more adsorption sites and increases the volumetric hydrogen uptake due to higher surface area per unit volume. The surface area of this novel structure can be maximized by decreasing the pore size without blocking the binding sites. For instance, PAF-11^[8] was expected to have the same structure as that of PAF-304 and exhibit significantly high hydrogen uptake. However, considering that no residue bromine was left after the complete formation of the framework, it can be safely concluded that partial interpenetration is responsible for the relatively low surface area and hydrogen uptake capacity. For smaller pore sizes, i.e., the pore size closer to the kinetic diameter of the guest molecules, the slow diffusion rate of guest molecules is a potential drawback. Porous materials with hierarchical pore dimensions are suitable candidates to resolve this issue. However, design and synthesis of hierarchical porous PAFs is a great challenge.

Although theoretical simulation studies can be used to refine the obtained experimental results and thus direct the synthesis of potential functional material, these solely depend on generation of models with proper geometrical and exact physical parameters. It is difficult to obtain the exact values of mentioned parameters for amorphous materials. The short-range order structure in PPNs and PAFs can be approximately considered as crystalline and can be used to predict their molecular adsorption behaviour. Experimental gas storage results on PAF-1^[1] coincide well with the simulation data obtained from the crystalline model, in fact, better than the amorphous model.^[32,39]

Pre-modification

Modification of PAF-1 with different functional groups or building blocks is another strategy to cater to the special application requirement. Both the pre-modification and PSM can implement functionalization on PAF-1^[1] with their own pros and cons. Pre-modification means designing functionalized monomer before the efficient and high-yielding cross-coupling reaction. The advantage of the pre-modification method is that it unblocks the pore in order to functionalize the parent material and effectively utilizes terminal groups to introduce specific units. With this strategy, heterocyclic building blocks such as tetrazole group in PIMs^[40], pyridyl and thiophenyl groups in PON-2 and PON-3 respectively^[6], B₃N₃ ring in BLP-12^[41] and perylene diimide in Td-PPI^[11] can be introduced into the PAF-1 framework. This enhances the interaction between host adsorbent and guest molecule by increasing the electron density of the framework. In particular, the interaction between an electrostatic ion of the heterocyclic rings and a quadrupole of CO₂ molecule is stronger than that between the π conjugated phenyl and a quadrupole of a CO₂ molecule. This makes the binding sites around heterocyclic rings more accessible to CO₂ molecules. Another pre-modification strategy is the introduction of a hybrid element to an alternative sp³ central carbon in the framework. Examples for addition could be Si in PAF-3^[4] and in [D4]PAF3^[42], Ge in PAF-4^[4] (also named as PPN-5^[27]), P⁺ in PP-Br^[5], and N⁺ in Ph₄N⁺F⁻^[43]. With the advantage of a stable and open framework, introduction of a hybrid element increases the structural diversity further expanding possible applications.

Post-synthesis modification (PSM)

PSM is superior and versatile owing to the possibility of incorporation of a wide variety of functional groups and controllable degree of modification. Introduction of polar functional groups and coordination sites to the framework mainly enhances the binding capacity. One example is the functionalization of PAF-1^[1] to increase CO₂ capture capacity. Considering the quadrupole moment of the CO₂ molecule, incorporation of polar functional groups into frameworks can effectively strengthen the separation efficacy of CO₂ over other non-polar or weakly polar molecules such as H₂, N₂, CH₄.

The PSM strategy used to modify PAF-1 is accomplished by incorporation of two moieties: 1) chemical functional groups as pendant units such as sulfonic acid^[3,44], hydroxyl^[45], alkyl- and amino-^[12] groups where lone pair donation and H-bonding improve the binding energy between CO₂ and cluster^[46]. 2) Metal doped into the open framework of PAF-1. Two preparation strategies that have been used for doping are: 1) vaporized fusion or mechanical mixing of the metal atoms with host material; 2) ion exchange or post-coordination of metal cation with the functional groups in the host skeleton. The former exposes more active sites but relatively lowers the stability of the host framework while the latter does just the opposite.^[47,48,49] However, chemical introduction of metal ions can prevent atoms from forming a cluster, actuate the design depending on the type and position of the doped metal and enhance the electrostatic field. Different doping methods are available as per the requirement of a specific application. Several factors should be considered before introduction of metals into the frameworks in order to enhance gas molecule sorption. For example, apart from the sorption affinity between gas molecules and the doped host framework, it is crucial to consider the affinity between the metal particles and host framework.

The other factors that need to be considered in the modification design process are as follows: 1) the weight of the metal ion or atom, 2) metal doping style and location in the framework, 3) gas molecule sorption location near the binding site, 4) the binding energy between metal particle and the gas molecules, 5) the degree of exposure of adsorption sites to gas molecules, 6) binding stability of metal within the host framework. The latter creates diminished stability if excess particles form clusters which reduce available surface.

Considering the above factors, alkali, alkaline-earth and transition metal ions and atoms are preferred for doping in porous organic frameworks to enhance gas sorption capacity. The multiscale simulation shows that the binding capacity of alkaline-earth metal atoms to the framework is weak while transition metal atoms is strong.^[47] It should be noted that if the binding capacity is of the order of chemisorption range it will suffer from desorption. Among the alkali metals, Na, K show low binding energy to organic frameworks and prefer to form clusters. The larger ionic radii of alkaline-earth metals have the binding stability problem. Li atom has light weight, binds to the framework in a stable fashion, and easily loses its valence electrons to form Li⁺ cation which in turn increases the electropositive force and the binding energy between the framework and gas molecules. Sun et al.'s calculation studies demonstrate that the lithium tetrazolide group is more stable and polarized than a Li atom doped into a porous organic framework.^[49] In addition, GCMC simulation predicts that the hydrogen gravimetric uptake of PAF-1 containing lithium tetrazolide moieties can exceed the 2010 DOE target and approaches to the 2015 US Department of Energy (DOE) target. One major drawback is its highly reactive and

flammable. Hence, there are substantial amounts of research on the gas sorption behaviour and property in the simulation stage but few experimental reports with the sample doped with lithium atom or ion in the porous framework. This is one of the biggest current challenges for synthetic chemists.

Carbonization

Carbonization of the framework is another effective functionalization method with enhanced gas sorption capacities. For example, direct annealing of PAF-1 at 450 °C shrinks the pore to a matching gas molecule dynamic diameter.^[16] KOH-activated carbonized PAF-1 exhibits a unique bimodal microporous structure.^[17] PAF-1 template carbon is another kind of porous material with high CO₂ binding capacity.^[50] It is prepared by introducing furfuryl alcohol into the PAF-1 framework followed by thermolysis at 900 °C. The pore size of PAF-1/C-900 decreased to 5.4 Å, and the CO₂ heat of sorption reached to 27 kJ mol⁻¹. Compared with PAF-1-450, the pores of the PAF-1/C-900/furfuryl have half the volume but retain equal surface and ability to adsorb CO₂.^[29]

Applications

CO₂ capture

Carbon capture and sequestration (CCS) of carbon released from industries and energy-related sources is deposited it for long term isolation from the atmosphere. Greenhouse gas carbon dioxide capture from power plants is one of the most important application areas of CCS. Although a power plant with CCS could reduce released CO₂ by 80% to 90%, the capture and compression of CO₂ requires 25% to 40% additional fuel which, in turn, increases the cost of electricity generation.^[51] There are mainly three different CO₂ capture systems: 1) pre-combustion removal of CO₂ from H₂ or CH₄ for clean energy fuel after the transformation of primary fuel (coal, natural gas, oil or biomass) into syngas (CO₂ and H₂ or CH₄) in the reactor; 2) post-combustion separation of CO₂ from flue gases after the combustion of primary fuel in air; 3) oxyfuel combustion which isolates CO₂ from water, the other combustion product.^[51] The components of flue gas in the post-combustion process are primarily nitrogen (N₂, >70%) and CO₂ (10-15%) which accounts for roughly 33-40% of global CO₂ emissions. In the post-combustion model, adsorption of CO₂ occurs at 1 bar and desorption occurs at 0.1 bar. In comparison with post-combustion carbon capture, the pre-combustion process is carried out at a higher pressure and also has a higher concentration of CO₂ 15-60%. The exhaust from oxygen combustion has a very high concentration of CO₂ requiring sorbents having stability in high humidity. The ideal CO₂ capture system should have sufficient space for CO₂ storage and appropriate binding capacity between CO₂ molecules and the sorbent material. Generally, large pore volume and high surface area contribute to high storage uptake, especially at high pressure range. Matching pore size with kinetic diameter (3.3 Å) of CO₂ and suitable binding energy leads to optimal interaction between the gas molecule and the material. In this regard, PAF-1 and its derivatives show potential for carbon dioxide capture when applied in pressure (PSA), temperature (TSA) or vacuum swing adsorption (VSA) systems. For improving CO₂ sorption capacity, carbonization, amination, metallization and sulfonation are four effective strategies.

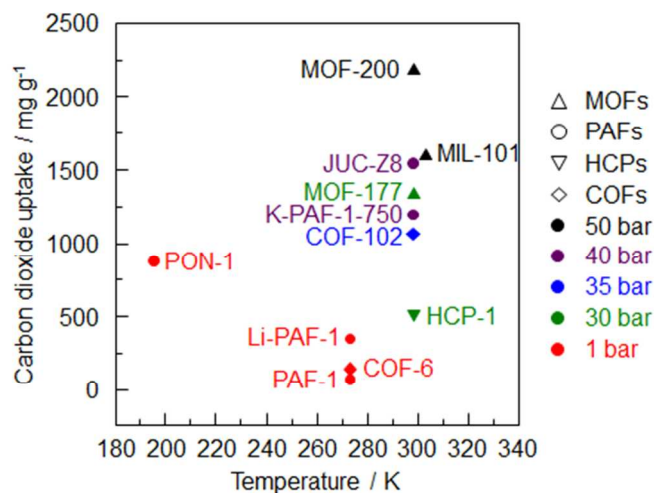


Figure 3. Summary of carbon dioxide uptake of porous organic frameworks vs. sorption temperature. (MOF-200^[26], MIL-101^[82], JUC-Z8^[95], MOF-177^[83], K-PAF-1-750^[17], COF-102^[24], PON-1^[6], HCP-1^[91], Li-PAF-1^[22], COF-6^[85], PAF-1^[11].)

In relating to PAF-1, carbonization follows two routes: either direct carbonization, annealing PAF-1 with hybrid compounds as template or fabrication of porous carbon with PAF-1 as a template. Generally, in an annealing process, framework shrink and pore size decrease contribute to the overlap of force fields and increase the interactions between carbon dioxide molecules and the framework.^[16] In addition, the all carbon scaffold possibly creates an electric field around the framework surface which strengthens its interaction with the quadrupole moment of CO₂. However, with a hard template, carbonized PAF-1 possesses both small and large pore.^[17] As a result, it shows a faster diffusion rate of guest molecules as well as higher CO₂ uptake in both low and high pressure range than that of PAF-1.

Amination is another useful strategy to introduce CO₂-philic moieties on porous organic frameworks. The polarizability and high charge density create stronger interaction between the network and quadrupole moment CO₂ molecules. For instance, PAF-1-CH₂NH₂ demonstrates the highest isosteric heat of sorption of 57.6 kJ mol⁻¹ among all PAF-1 derivatives equalling that of chemical sorption.^[12] (Table S2) However, the strong interaction demands more energy to regenerate. Notably, as the Q_{st} increases, it becomes less satisfactory. It has been shown that material with Q_{st} around 21 kJ mol⁻¹ exhibits the best working capacity in landfill gas separation via a PSA process.^[52] However, in real world applications, CO₂ sorption is usually combined with water vapour even in pre- or post-combustion processes. Stability of the above mentioned derivatives in the presence of water vapour should be considered. It has been reported that all the amine-containing materials are deactivated at different rates compared with urea under humid conditions. Deactivation does not occur in dry CO₂ adsorption conditions.^[53]

Metal cation in the framework acts as an open coordination site after full activation, which leads to stronger electrostatic interactions between CO₂ and the metal cation.^[3,13,15,111,112] Light element Li is a commonly used dopant. However, the Li content should be present in an appropriate optimum range. If one Li ion is present per phenyl ring, the Li content is as high as 8 % weight. Extremely high loading levels of Li will make

the lithium ions agglomerate and degrade the framework and lead to diminished CO₂ sorption capacity. Introduction of Ni in the framework by coordination interaction with porphyrin has been proven to enhance CO₂ sorption capacity.^[15]

In the case of sulfonate grafted porous polymer networks two factors enhance the CO₂-philic effect of the materials.^[3] First, functionalization of all-carbon-scaffold frameworks creates electric fields on the surface that impart a strong affinity of the networks towards CO₂ molecules by their high quadrupole moment. Second, small pore size and polar functionalities increase the heat of adsorption. Accurate control of the amount and location of sulfonate molecules is the same whether performed before or after the polymerization.^[44,54] Other hybrid elements, such as Si in PAF-3^[4] (also known as PPN-4,^[27] network 2^[2]), Ge in PAF-4,^[4] P in PP-Br,^[5] S in PON-3,^[6] B in BLP,^[41,55] have been studied for their influence on host-guest interaction. Increases of different degrees are seen in carbon dioxide enthalpy. (Table S2)

Comparing of four kinds of modification strategies, amination is the most effective method to improve the carbon dioxide sorption enthalpy and PPN-6-CH₂DETA^[56] demonstrates the highest uptake at room temperature and 1 bar of all the polyamine-tethered PPNs. With increased affinity of carbon dioxide, the affinity of other gases increases too. Selectivity is another indicator of ideal carbon dioxide sorbent. PPN-6-CH₂DETA exhibits the highest CO₂/N₂ selectivity based on the IAST method. It should be noted that a sample with ultrahigh surface area has an absolute advantage in high pressure carbon dioxide capture. MOF-200 with the highest uptake is the best example. (Fig. 3) Considering the stability and the storage capacity, PAF-1 and its derivatives are the best CO₂ adsorbents among porous organic frameworks.

H₂ storage

Hydrogen with energy content of 142 MJ kg⁻¹ is the environmentally friendly energy storage medium in hydrogen economy. However, the safe transfer and cost-effectiveness of storage of H₂ is still a big challenge in terms of application. The practical 2015 requirement of the U.S. Department of Energy (DOE) sets a storage standard (5.5 wt% in gravimetric capacity, 40 g L⁻¹ of volumetric capacity between 233 to 333 K).^[57] With the aid of chemical bonds, hydrides can adsorb as much as the target set by DOE under ambient conditions.^[58] But the strong interactions require high temperature for hydrogen release, which makes recycling unavailable. For instance, the promising one, MgH₂, requires over 350 °C to release hydrogen. In addition, the metal hydride is generally too heavy to gravimetric hydrogen uptake. Hence, lowering desorption temperature and improving the amount of gravimetric adsorption is a big challenge in chemisorption of hydrogen. On the other hand, reversible physisorption allows recycling due to the weak van der Waals forces between the host and guest, requiring very low temperature to make kinetics faster and store significant amounts of hydrogen. The challenge for hydrogen storage with physical interaction is how to increase the gas uptake at ambient conditions. Fortunately, although MOFs and PAFs exhibit similar volumetric amounts of hydrogen, greater gravimetric uptake can be expected due to the light element framework and low density in PAF-1.

PAF-1 adsorbs hydrogen of 186 cm³ g⁻¹ (1.66 wt%) at 77 K/1 bar, and 75.3 mg g⁻¹ (7 wt%) at 77 K/48 bar.^[11] (Table S2) However, this value decreases dramatically as the temperature rises and pressure drops. To achieve the DOE target, high hydrogen uptake at close to ambient temperature and at lower pressure range is required. In this regard, improving the hydrogen binding energy of the framework is one of the breakthroughs to resolve this issue. There are three main forces (dispersion interactions, electrostatic interactions, and orbital interactions) between hydrogen molecules and the adsorbent, which directly determine the strength of the binding energy.^[59] The ideal enthalpy for adsorbent should be 15-25 kJ mol⁻¹.^[60] However, Froudakis et al. revealed that binding energy between phenyl rings and hydrogen molecule is less than 1 kcal mol⁻¹, corresponds with 4.18 kJ mol⁻¹.^[61] Moreover, weaker liquid-liquid interaction in empty spaces of the large pore makes the enthalpy decrease with increase in the coverage, which reduces the overall hydrogen uptake.^[62] Generally, introduction of a functional group or metal element partly blocks the channel narrowing the pore to match the size of the hydrogen kinetic diameter. Significant charge/quadrupole or charge/induced-dipole interaction between metal ions and hydrogen molecules enhances the binding energy.^[45]

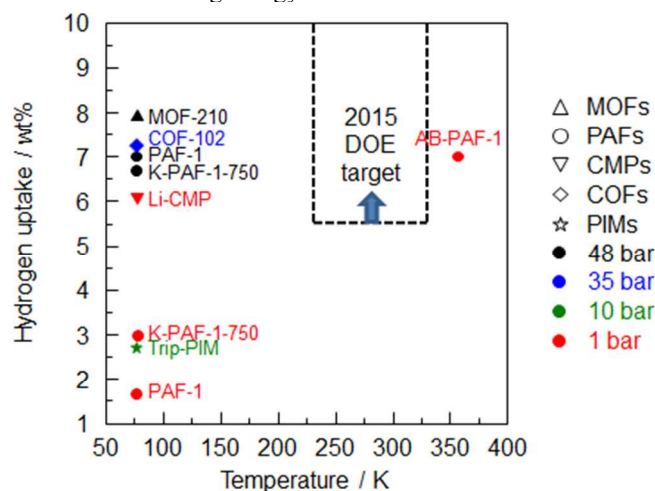


Figure 4. Summary of hydrogen uptake of porous organic frameworks vs. sorption temperature. (MOF-210^[26], COF-102^[24], PAF-1^[11], K-PAF-1-750^[17], Li-CMP^[87], Trip-PIM^[94], AB-PAF-1^[63].)

Substantiated by experimental results, lithiation,^[13] carbonization^[16,17] and nickel coordination^[15] are three effective methods to enhance the hydrogen heat of sorption. It is found that Li is one of the most ideal elements doped in the framework. PAF-1 lithiated with naphthalene shows the hydrogen adsorption enthalpy as high as 9 kJ mol⁻¹. PAF-1 lithiated with naphthalene shows the highest hydrogen adsorption enthalpy of 9 kJ mol⁻¹ among all PAF-1 and its derivatives. (Table S2)

Until now, MOF-210^[26] exhibited the highest hydrogen uptake in high pressure (48 bar), while Li-CMP^[87] shows the highest value in low pressure (1 bar) among porous organic frameworks. (Fig. 4) Unfortunately, none of them reach the DOE target. One can expand hydrogen sorption by adopting a new strategy involving a combination of high surface area and pore volume PAF-1 with high stoichiometric hydrogen content (19.6 wt %) and moderate dehydrogenation temperature using ammonia borane (AB).^[63] As expected, hydrogen release is substantial improved by AB-PAF-1 which operates at a

temperature of 358 K compared with the 77 K operating temperature of other porous organic frameworks. Moreover, nano-dispersed AB in PAF-1 provides a method to increase the hydrogen gravimetric capacity which is an important aspect to consider in chemical hydrogen storage processes.

CH₄ storage

Methane benefits from its high gravimetric heat of combustion (55.7 MJ kg⁻¹ compared with 46.4 MJ kg⁻¹ of gasoline), smallest amount of CO₂ release per unit of heat produced among fossil fuels and large natural reserves. This makes methane an attractive fuel option in cars and other automobiles as an alternative to petroleum-based fuels. DOE initiated a methane storage program with 0.5 g_{methane}/g_{sorbent} for gravimetric capacity requirement and 263 v_{methane} (STP)/v_{sorbent} for volumetric capacity requirement. Considering 25% packing loss, the volumetric capacity should be up to 330 v_{methane} (STP)/v_{sorbent}.^[64] In addition, the ideal sorbent should be stable to the impurity species in natural gas sources with a lifetime of at least 100 adsorption-desorption cycles.

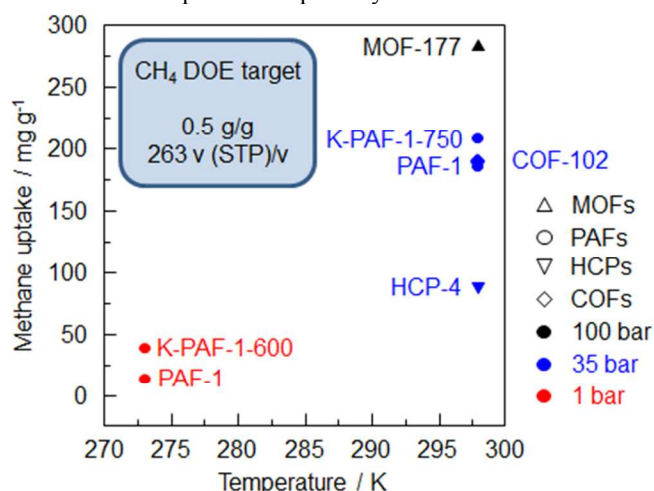


Figure 5. Summary of methane uptake of porous organic frameworks vs. sorption temperature. (K-PAF-1-750^[17], PAF-1^[1], HCP-4^[91], K-PAF-1-600^[17], COF-102^[24])

The adsorption behaviour of methane on adsorbents is the same as that of hydrogen. The physisorption mainly depends on surface area, pore volume and affinity towards methane and it is preferred to chemisorption due to its reversible nature. However, it does not mean larger surface area would ensure better adsorption. It has been calculated for MOFs that the gravimetric uptake increases with increase in surface area up to 2500–3000 m² g⁻¹; above this point, the only effect is a decrease in volumetric uptake.^[65] Only until the measurement pressure exceeds 100 bar, the accessible volume plays a major role in methane storage. In this case, the effect of adsorbent is minimal, almost equivalent to the directly compressed methane at the same pressure.^[65] Van der Waal force is the driving force in physisorption. Tuning the pore size in order to match with one or two kinetic diameters (3.8 Å) of methane is the optimal strategy. Incorporation of large amount of aromatic building blocks or electron-donating species improves methane uptake because of enhanced electrostatic interaction. For example, the statistical simulation results from 137953 hypothetical MOFs shows that methyl, ethyl and propyl functional groups could dramatically improve the methane uptake over 205 v_{methane}

(STP)/v_{sorbent}.^[65] Methane uptake can also be improved by lithiation of PAF-1 and its derivatives. London dispersion and induced dipole interactions between Li⁺ cation and methane molecule can strengthen the binding capacity.^[66] For example, the methane uptake of 5% Li-PAF-1 is 20.8 mg g⁻¹, which is about twice higher than that of PAF-1 under the same conditions (273 K/1 bar).^[14] Fortunately, the heat of methane sorption is reasonable, but enhancement of the packing density and amount of desorption pose two main challenges that need to be addressed.

PAF-1 can adsorb 185 mg g⁻¹ CH₄ at 298 K/35 bar, but this value is still far away from the DOE target. (Fig. 5) Even PPN-4^[27] which shows the highest methane uptake of 273.6 mg g⁻¹ (295 K/35 bar) among PAF-1 derivatives can't reach the DOE target. (Table S2) The volumetric uptake calculated for PPN-4 with network density of 0.2 g cm⁻³ is only 77 v/v. Fortunately, PPN-4 can be compressed to half of its volume without significant loss of porosity in order to improve density and volumetric uptake.^[67] Thus, it can be concluded that excessively large pores are not mandatory for high methane volumetric uptake capacity. Additionally, the interaction between methane and pore surface area decreases with increase in surface coverage, possibly because the excessive space cannot be effectively utilized for methane loading.

Small hydrocarbon molecule sorption

C₁ to C₃ light hydrocarbons (CH₄, C₂H₂, C₂H₄, C₂H₆, C₃H₆ and C₃H₈) are very important raw materials for industrial products and fine chemicals. Cryogenic distillation is the traditional large scale technology implemented for separation of these chemicals. From an energy saving point of view, adsorption separation with solid sorbents stands as a potential alternative technology owing to the high operating temperature. Porous organic frameworks characterized with tunable pore size for molecule selective sieving and functionalized frameworks for specific recognition molecules attract attention. Based on the combined simulated breakthrough research, involving IAST experiments, single component gas sorption measurements on several MOFs^[68-73], three conclusions can be made. First, van der Waals forces predominate in the interaction between MOFs and hydrocarbon molecules, so the longer the hydrocarbon chain the greater the interaction capacity.^[71] As expected, methane shows weaker interaction than C₂, C₃ hydrocarbons and, so, can be easily separated. Second, high density of open metal sites in MOFs plays an important role in separation of light hydrocarbons.^[68] It suggests that, based on the high surface area and pore volume, immobilized PAF-1 or its derivatives with different functional sites such as open metal sites, -NH₂, -OH, and Lewis pyridine sites can enhance the selectivity of alkyl, olefin, and alkyne chains. Third, a chemically robust framework is essential. MCOF-1 is one of the few examples about PAF-1 derivatives applied in light hydrocarbons separation.^[74] By gas sorption measurements at 273 K and 298 K, 1 bar, zero-point Q_{st} of MCOF-1 was calculated to be 15 kJ mol⁻¹ for CH₄, and 41 kJ mol⁻¹ for C₂H₆, which is around three times higher than CH₄. By means of IAST method, it was found that the selectivity for MCOF is 1800 for C₃H₈/CH₄, 88 for C₂H₆/CH₄, and 26 for C₂H₄/CH₄. The latter two values surpass the corresponding values of the previously reported porous adsorbents.

Other small molecule recognition

Small molecule recognition of PAF-1 derivatives results from its different binding capacities with different molecules. Generally, the interactions between host frameworks and molecules are non-covalent in nature such as hydrogen bonding, metal coordination, hydrophobic forces, van der Waals forces, π - π interactions, and electrostatic and/or electromagnetic effects.^[44,75,76] To detect the binding intensity, several methods such as single component sorption measurements,^[1,8] spectroscopy,^[77] chromatography,^[77] and breakthrough^[10,78] have been implemented. PAF-1 can adsorb large amounts of benzene and toluene vapour at 298 K/1 bar; the value is as high as 1306 mg g⁻¹, and 1357 mg g⁻¹ respectively.^[1] Substantiated by theoretical analysis, all of the PAF-1 derivatives^[8,38,79,80] contain aromatic building blocks which are advantageous for selective recognition of small aromatic hydrocarbons from aliphatic hydrocarbons due to the π - π interactions in the aromatic rings. Tuning the hydrophilic-hydrophobic ratio of the channel with sulfonate groups makes the material recognize small molecules with different polarity.^[44] On the other hand, PAF-1 derivatives could be used to detect toxic small molecules. Examples are: ammonia, octane, cyanogen chloride and sulphur dioxide,^[10] nuclear waste iodine under dry and humid vapour conditions or in solvent system;^[77] organic small molecules such as methanol and chloroform in n-hexane solvent.^[77]

Three conclusions are summarized here. First, a large surface area of material leads to high small molecule uptake. Second, nonselective pore size decrease enhances the affinity between all guest molecules and the network. Third, the increased content of aromatic building blocks and the specific functional groups modified on PAF-1 improve the binding capacity to particular molecules which strengthen selective recognition.

Conclusion and outlook

The synthesis of PAF-1 was inspired by its classic porous contemporaries such as zeolites^[81], metal-organic frameworks (MOFs)^[26,28,82,83], covalent organic frameworks (COFs)^[24,84,85], conjugated microporous polymers (CMPs)^[86,87,88], hyper-crosslinked polymers (HCPs)^[89,90,91], triazine-based organic frameworks (CTFs)^[92], porous aromatic frameworks (PAFs)^[1,4,8,110] and polymers of intrinsic microporosity (PIMs)^[93,94]. PAF-1 and its derivatives exhibit impressive properties and, therefore, attract great attention. Diversity of building blocks and a variety of synthetic methods give rise to this series of materials with different structures and functions. It can be confirmed that the nature of materials is determined by the synergy between various factors and parameters, which is aptly described by Snurr and co-workers as “only one structure characteristic has to be wrong for a material to perform poorly, but many characteristics must be optimal for a material to perform well”.^[50]

For future contestation, a co-condensation reaction using tetrahedron building blocks and other types of units is an attractive method for synthesizing advanced functional materials. For example, condensation with tetrahedron TBPM and triangle TBPA in different ratios can give a series of porous organic frameworks named as C-POFs.^[95] All of these retain the advantage of PAF-1, but show stronger binding capacity as in JUC-Z2. Compared with PAF-1 and JUC-Z2, the C-POFs show excellent low-pressure gas uptake and high-pressure gas storage capacity.

In addition, the hybrid building blocks can be pre- or post-functionalized to construct novel structures thus expanding

their potential applications in catalysis.^[96-99] Catechol-functionalized porous organic polymers which are synthesized by cobalt-catalysed acetylene trimerization (CCAT) strategy attract much attention in this area. Modified PAF-1 exhibits broad prospects in catalysis for three reasons: 1) PAF-1 and its derivatives constructed with covalent bonds and highly cross-linked frameworks lead to high physicochemical stability even in some harsh conditions (acid, base or organic solvent system); 2) PAF-1 and its derivatives possess designable structures, porosities, and functionalities, which can satisfy the various activity and selectivity requirements of a specific catalytic reaction; 3) High surface area and physical separation of coordinating groups can stabilize and isolate catalytically active metal sites.

The large free volume and robust light architecture of porous organic frameworks not only act as storage capsules for molecules,^[100] but also provide an ideal venue for molecular rotor operation.^[101] The p-phenylene groups in deuterated PAF-3 spin at ultrafast speed, even at temperatures as low as 200 K.^[42] In particular, the rotor dynamics can be regulated by guest molecules which easily diffuse around the open framework. The intensive dynamics makes these kinds of materials suitable for engineering oscillating dipoles. Moreover, their sensitive responses to chemical stimuli make these porous polymers suitable candidates for responsive materials with switchable ferroelectricity and for applications in devices such as sensors, and actuators which require capture and release of chemicals on command.

Acknowledgements

This work was supported by the National Basic Research Program of China (2011CB808703, 2012CB821700), National Natural Science Foundation of China (Grant nos. 91022030, 21261130584, 21390394), “111” project (B07016), Award Project of KAUST (CRG-1-2012-LAI-009) and Ministry of Education, Science and Technology Development Center Project (20120061130012).

Notes and references

^a State Key Laboratory of Inorganic Synthesis and Preparative Chemistry, Jilin University, Changchun, China.

^b Department of Chemistry, Jilin University, Changchun, China.

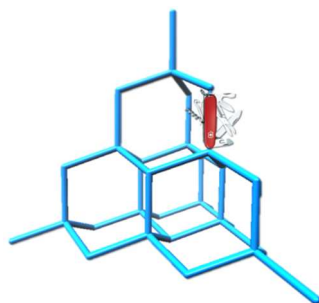
* sqiu@jlu.edu.cn; then@jlu.edu.cn

Electronic Supplementary Information (ESI) available: [details of any supplementary information available should be included here]. See DOI: 10.1039/b000000x/

- 1 T. Ben, H. Ren, S. Ma, D. Cao, J. Lan, X. Jing, W. Wang, J. Xu, F. Deng, J. M. Simmons, S. Qiu and G. Zhu, *Angew. Chem. Int. Ed.*, 2009, **48**, 9457.
- 2 J. R. Holst, E. Stöckel, D. J. Adams and A. I. Cooper, *Macromolecules*, 2010, **43**, 8531.
- 3 W. Lu, D. Yuan, J. Sculley, D. Zhao, R. Krishna and H. Zhou, *J. Am. Chem. Soc.*, 2011, **133**, 18126.
- 4 T. Ben, C. Pei, D. Zhang, J. Xu, F. Deng, X. Jing and S. Qiu, *Energy Environ. Sci.*, 2011, **4**, 3991.
- 5 Zhang, S. Zhang and S. Li, *Macromolecules*, 2012, **45**, 2981.
- 6 H. J. Jeon, J. H. Choi, Y. Lee, K. M. Choi, J. H. Park and J. K. Kang, *Adv. Energy Mater.*, 2012, **2**, 225.
- 7 R. Dawson, E. Stöckel, J. R. Holst, D. J. Adams and A. I. Cooper, *Energy Environ. Sci.*, 2011, **4**, 4239.

8. Y. Yuan, F. Sun, H. Ren, X. Jing, W. Wang, H. Ma, H. Zhao and G. Zhu, *J. Mater. Chem.*, 2011, **21**, 13498.
9. M. G. Rabbani and H. M. El-Kaderi, *Chem. Mater.*, 2012, **24**, 1511.
10. G. W. Peterson, O. K. Farha, B. Schindler, P. Jones, J. Mahle and J. T. Hupp, *J. Porous Mater.*, 2012, **19**, 261.
11. K. V. Rao, R. Haldar, C. Kulkarni, T. K. Maji and S. J. George, *Chem. Mater.*, 2012, **24**, 969.
12. S. J. Garibay, M. H. Weston, J. E. Mondloch, Y. J. Colón, O. K. Farha, J. T. Hupp and S. T. Nguyen, *CrystEngComm*, 2013, **15**, 1515.
13. H. Ma, H. Ren, X. Zou, F. Sun, Z. Yan, K. Cai, D. Wang and G. Zhu, *J. Mater. Chem. A*, 2013, **1**, 752.
14. K. Konstas, J. W. Taylor, A. W. Thornton, C. M. Doherty, W. X. Lim, T. J. Bastow, D. F. Kennedy, C. D. Wood, B. J. Cox, J. M. Hill, A. J. Hill and M. R. Hill, *Angew. Chem. Int. Ed.*, 2012, **51**, 6639.
15. Z. Wang, S. Yuan, A. Mason, B. Reprogle, D. Liu and L. Yu, *Macromolecules*, 2012, **45**, 7413.
16. T. Ben, Y. Li, L. Zhu, D. Zhang, D. Cao, Z. Xiang, X. Yao and S. Qiu, *Energy Environ. Sci.*, 2012, **5**, 8370.
17. Y. Li, T. Ben, B. Zhang, Y. Fu and S. Qiu, *Scientific Reports*, 2013, **3**, 2420.
18. T. Yamamoto, *Bull. Chem. Soc. Jpn.*, 1999, **72**, 621.
19. G. Zhou, M. Baumgarten and K. Müllen, *J. Am. Chem. Soc.*, 2007, **129**, 12211.
20. A. B. Cairns and A. L. Goodwin, *Chem. Soc. Rev.*, 2013, **42**, 4881.
21. N. B. McKeown and P. M. Budd, *Macromolecules*, 2010, **43**, 5163.
22. R. L. Martin, M. N. Shahrak, J. A. Swisher, C. M. Simon, J. P. Sculley, H. Zhou, B. Smit and M. Haranczyk, *J. Phys. Chem. C*, 2013, **117**, 20037.
23. H. Jiang, T. A. Makal and H. Zhou, *Coord. Chem. Rev.*, 2013, **257**, 2232.
24. H. M. El-Kaderi, J. R. Hunt, J. L. Medoza-Cortés, A. P. Côté, R. E. Taylor, M. O’Keeffe and O. M. Yaghi, *Science*, 2007, **316**, 268.
25. N. T. T. Nguyen, H. Furukawa, F. Gándara, H. T. Nguyen, K. E. Cordova and O. M. Yaghi, *Angew. Chem. Int. Ed.*, 2014, DOI: 10.1002/anie.201403980.
26. H. Furukawa, N. Ko, Y. B. Go, N. Aratani, S. B. Choi, E. Choi, A. Ö. Yazaydin, R. Q. Snurr, M. O’Keeffe, J. Kim and O. M. Yaghi, *Science*, 2010, **329**, 424.
27. D. Yuan, W. Lu, D. Zhao and H. Zhou, *Adv. Mater.*, 2011, **23**, 3723.
28. O. K. Farha, I. Eryazici, N. C. Jeong, B. G. Hauser, C. E. Wilmer, A. A. Sarjeant, R. Q. Snurr, S. T. Nguyen, A. Ö. Yazaydin and J. T. Hupp, *J. Am. Chem. Soc.*, 2012, **134**, 15016.
29. V. Presser, J. McDonough, S. Yeon and Y. Gogotsi, *Energy Environ. Sci.*, 2011, **4**, 3059.
30. Y. Yan, I. Telepeni, S. Yang, X. Lin, W. Kockelmann, A. Dailly, A. J. Blake, W. Lewis, G. S. Walker, D. R. Allan, S. A. Barnett, N. R. Champness and M. Schröder, *J. Am. Chem. Soc.*, 2010, **132**, 4092.
31. L. Huang and D. Cao, *J. Mater. Chem. A*, 2013, **1**, 9433.
32. J. Lan, D. Cao, W. Wang, T. Ben and G. Zhu, *J. Phys. Chem. Lett.*, 2010, **1**, 978.
33. Z. Yang, X. Peng and D. Cao, *J. Phys. Chem. C*, 2013, **117**, 8353.
34. B. Lukose, M. Wahiduzzaman, A. Kuc and T. Heine, *J. Phys. Chem. C*, 2012, **116**, 22878.
35. A. F. Oliveira, G. Seifert, T. Heine and H. A. Duarte, *J. Brazil. Chem. Soc.*, 2009, **20**, 1193.
36. G. Seifert, D. Porezag and T. Frauenheim, *Int. J. Quantum. Chem.*, 1996, **58**, 185.
37. S. Patchkovskii and T. Heine, *Phys. Rev. E*, 2009, **80**, 031603.
38. H. Ren, T. Ben, E. Wang, X. Jing, M. Xue, B. Liu, Y. Cui, S. Qiu and G. Zhu, *Chem. Commun.*, 2010, **46**, 291.
39. R. Babarao, S. Dai and D. E. Jiang, *Langmuir*, 2011, **27**, 3451.
40. N. Y. Du, H. B. Park, G. P. Robertson, M. M. Dal-Cin, T. Visser, L. Scoles and M. D. Guiver, *Nat. Mater.*, 2011, **10**, 372.
41. K. T. Jackson, M. G. Rabbani, T. E. Reich and H. M. El-Kaderi, *Polym. Chem.*, 2011, **2**, 2775.
42. A. Comotti, S. Bracco, T. Ben, S. Qiu and P. Sozzani, *Angew. Chem. Int. Ed.*, 2014, **126**, 1061.
43. A. Trewin, G. R. Darling and A. I. Cooper, *New J. Chem.*, 2008, **32**, 17.
44. Y. Yang, Q. Zhang, Z. Zhang and S. Zhang, *J. Mater. Chem. A*, 2013, **1**, 10368.
45. M. H. Weston, O. K. Farha, B. G. Hauser, J. T. Hupp and S. T. Nguyen, *Chem. Mater.*, 2012, **24**, 1292.
46. Z. Xiang and D. Cao, *J. Mater. Chem. A*, 2013, **1**, 2691.
47. J. Lan, D. Cao, W. Wang and B. Smit, *ACS Nano*, 2010, **4**, 4225.
48. L. Wang, Y. Sun and H. Sun, *Faraday Discuss.*, 2011, **151**, 143.
49. Y. Sun, T. Ben, L. Wang, S. Qiu and H. Sun, *J. Phys. Chem. Lett.*, 2010, **1**, 2753.
50. Y. Zhang, B. Li, K. Williams, W. Gao and S. Ma, *Chem. Commun.*, 2013, **49**, 10269.
51. [IPCC, 2005] *IPCC special report on Carbon Dioxide Capture and Storage*. Prepared by working group III of the Intergovernmental Panel on Climate Change. B. Metz, O. Davidson, H. C. de Coninck, M. Loos and L. A. Meyer, Cambridge University Press, Cambridge, United Kingdom and New York, USA, 442.
52. C. E. Wilmer, O. K. Farha, Y. Bae, J. T. Hupp and R. Q. Snurr, *Energy Environ. Sci.*, 2012, **5**, 9849.
53. A. Sayari, A. Heydari-Gorji and Y. Yang, *J. Am. Chem. Soc.*, 2012, **134**, 13834.
54. Z. Zhang, L. Wu and T. Xu, *J. Mater. Chem.*, 2012, **22**, 13996.
55. T. E. Reich and H. M. El-Kaderi, *J. Nanopart Res.*, 2013, **15**, 1368.
56. W. Lu, J. P. Sculley, D. Yuan, R. Krishna, Z. Wei and H. Zhou, *Angew. Chem. Int. Ed.*, 2012, **51**, 7480.
57. DOE. U.S. Department of Energy, “Target for onboard hydrogen storage systems for light-duty vehicles,” 2012, http://www1.eere.energy.gov/hydrogenandfuelcells/storage/pdfs/targets_onboard_hydro_storage.pdf
58. Z. Li, G. Zhu, G. Lu, S. Qiu and X. Yao, *J. Am. Chem. Soc.*, 2010, **132**, 1490.
59. R. C. Lochan and M. Head-Gordon, *Phys. Chem. Chem. Phys.*, 2006, **8**, 1357.
60. A. W. C. van den Berg and C. O. Areán, *Chem. Commun.*, 2008, 668.
61. E. Klontzas, E. Tylianakis and G. E. Froudakis, *J. Phys. Chem. C*, 2008, **112**, 9095.
62. S. B. Kalidindi and R. A. Fischer, *Phys. Status Solidi. B*, 2013, **250**, 1119.
63. Y. Peng, T. Ben, Y. Jia, D. Yang, H. Zhao, S. Qiu and X. Yao, *J. Phys. Chem. C*, 2012, **116**, 25694.
64. Y. Peng, V. Krungleviciute, I. Eryazici, J. T. Hupp, O. K. Farha and T. Yildirim, *J. Am. Chem. Soc.*, 2013, **135**, 11887.

65. C. E. Wilmer, M. Leaf, C. Y. Lee, O. K. Farha, B. G. Hauser, J. T. Hupp and R. Q. Snurr, *Nat. Chem.*, 2012, **4**, 83.
66. J. Lan, D. Cao and W. Wang, *Langmuir*, 2009, **26**, 220.
67. T. A. Makal, J. Li, W. Lu and H. Zhou, *Chem. Soc. Rev.*, 2012, **41**, 7761.
68. Y. He, R. Krishna and B. Chen, *Energy Environ. Sci.*, 2012, **5**, 9107.
69. E. D. Bloch, W. L. Queen, R. Krishna, J. M. Zadrozny, C. M. Brown and J. R. Long, *Science*, 2012, **335**, 1606.
70. Y. He, Z. Zhang, S. Xiang, H. Wu, F. R. Fronczek, W. Zhou, R. Krishna, M. O'Keeffe and B. Chen, *Chem-Eur. J.*, 2012, **18**, 1901.
71. Y. He, Z. Zhang, S. Xiang, F. R. Fronczek, R. Krishna and B. Chen, *Chem. Commun.*, 2012, **48**, 6493.
72. J. Duan, M. Higuchi, S. Horike, M. L. Foo, K. P. Rao, Y. Inubushi, T. Fukushima and S. Kitagawa, *Adv. Funct. Mater.*, 2013, **23**, 3525.
73. H. Xu, B. Chen and G. Qian, *J. Mater. Chem. A*, 2013, **1**, 9916.
74. H. Ma, H. Ren, S. Meng, Z. Yan, H. Zhao, F. Sun and G. Zhu, *Chem. Commun.*, 2013, **49**, 9773.
75. A. Dhotel, Z. Chen, L. Delbreilh, B. Youssef, J. Saiter and L. Tan, *Int. J. Mol. Sci.*, 2013, **14**, 2303.
76. B. Moulton and M. J. Zaworotko, *Chem. Rev.*, 2001, **101**, 1629.
77. C. Pei, T. Ben, S. Xu and S. Qiu, *J. Mater. Chem. A*, 2014, **2**, 7179.
78. A. Torres-Knoop, R. Krishna and D. Dubbeldam, *Angew. Chem. Int. Ed.*, 2014, **53**, 7774.
79. V. R. Pedireddi, S. Chatterjee, A. Ranganathan and C. N. R. Rao, *J. Am. Chem. Soc.*, 1997, **119**, 10867.
80. A. Ranganathan, V. R. Pedireddi, S. Chatterjee and C. N. R. Rao, *J. Mater. Chem.*, 1999, **9**, 2407.
81. M. E. Davis, *Nature*, 2002, **417**, 813.
82. P. L. Llewellyn, S. Bourrelly, C. Serre, A. Vimont, M. Daturi, L. Hamon, G. D. Weireld, J. Chang, D. Hong, Y. K. Hwang, S. H. Jung and G. Férey, *Langmuir*, 2008, **24**, 7245.
83. D. Saha, Z. Bao, F. Jia, and S. Deng, *Environ. Sci. Technol.*, 2010, **44**, 1820.
84. A. P. Côté, A. I. Benin, N. W. Ockwig, M. O'Keeffe, A. J. Matzger and O. M. Yaghi, *Science*, 2005, **310**, 1166.
85. H. Furukawa, and O. M. Yaghi, *J. Am. Chem. Soc.*, 2009, **131**, 8875.
86. J. Jiang, F. Su, A. Trewin, C. D. Wood, N. L. Campbell, H. Niu, C. Dickinson, A. Y. Ganin, M. J. Rosseinsky, Y. Z. Khimyak and A. I. Cooper, *Angew. Chem. Int. Ed.*, 2007, **46**, 8574.
87. S. Wan, J. Guo, J. Kim, H. Ihee and D. Jiang, *Angew. Chem. Int. Ed.*, 2008, **47**, 8826.
88. A. Li, R. Lu, Y. Wang, X. Wang, K. Han, and W. Deng, *Angew. Chem. Int. Ed.*, 2010, **49**, 3330.
89. C. D. Wood, B. Tan, A. Trewin, H. Niu, D. Bradshaw, M. J. Rosseinsky, Y. Z. Khimyak, N. L. Campbell, R. Kirk, E. Stöckel and A. I. Cooper, *Chem. Mater.*, 2007, **19**, 2034.
90. M. P. Tsyurupa and V. A. Davankov, *React. Funct. Polym.*, 2002, **53**, 193.
91. C. F. Martin, E. Stöckel, R. Clowes, D. J. Adams, A. I. Cooper, J. J. Pis, F. Rubiera and C. Pevida, *J. Mater. Chem.*, 2011, **21**, 5475.
92. J. Schmidt, M. Werner and A. Thomas, *Macromolecules*, 2009, **42**, 4426.
93. N. B. McKeown, and P. M. Budd, *Chem. Soc. Rev.*, 2006, **35**, 675.
94. B. S. Ghanem, K. J. Msayib, N. B. McKeown, K. D. M. Harris, Z. Pan, P. M. Budd, A. Butler, J. Selbie, D. Book, and A. Walton, *Chem. Commun.*, 2007, 67.
95. C. Pei, T. Ben, Y. Li and S. Qiu, *Chem. Commun.*, 2014, **50**, 6134.
96. S. J. Kraft, R. H. Sánchez and A. S. Hock, *ACS Catal.*, 2013, **3**, 826.
97. K. K. Tanabe, N. A. Siladke, E. M. Broderick, T. Kobayashi, J. F. Goldston, M. H. Weston, O. K. Farha, J. T. Hupp, M. Pruski, E. A. Mader, M. J. A. Johnson and S. T. Nguyen, *Chem. Sci.*, 2013, **4**, 2483.
98. Z. Xie, C. Wang, K. E. deKrafft and W. Lin, *J. Am. Chem. Soc.*, 2011, **133**, 2056.
99. P. Kaur, J. T. Hupp and S. T. Nguyen, *ACS Catal.*, 2011, **1**, 819.
100. A. Comotti, S. Bracco, M. Mauri, S. Mottadelli, T. Ben, S. Qiu and P. Sozzani, *Angew. Chem. Int. Ed.*, 2012, **51**, 10136.
101. A. Comotti, S. Bracco, P. Valsesia, M. Beretta and P. Sozzani, *Angew. Chem. Int. Ed.*, 2010, **49**, 1760.
102. Y. Yang, Q. Zhang, J. Zheng and S. Zhang, *Polymer*, 2013, **54**, 3254.
103. H. A. Patel, S. H. Je, J. Park, D. P. Chen, Y. Jung, C. T. Yavuz and A. Coskun, *Nat. Commun.*, 2013, **4**, 1357.
104. P. Pandey, O. K. Farha, A. M. Spokoyny, C. A. Mirkin, M. G. Kanatzidis, J. T. Hupp and S. T. Nguyen, *J. Mater. Chem.*, 2011, **21**, 1700.
105. H. Zhao, Z. Jin, H. Su, J. Zhang, X. Yao, H. Zhao and G. Zhu, *Chem. Commun.*, 2013, **49**, 2780.
106. D. Zhang, Z. Chang, Y. Lv, T. Hu and X. Bu, *RSC Adv.*, 2012, **2**, 408.
107. H. Qian, J. Zheng and S. Zhang, *Polymer*, 2013, **54**, 557.
108. W. Lu, D. Yuan, D. Zhao, C. I. Schilling, O. Plietzsch, T. Muller, S. Bräse, J. Guenther, J. Blümel, R. Krishna, Z. Li and H. Zhou, *Chem. Mater.*, 2010, **22**, 5964.
109. E. Stöckel, X. Wu, A. Trewin, C. D. Wood, R. Clowes and A. I. Cooper, *Chem. Commun.*, 2009, 212.
110. T. Ben and S. Qiu, *CrystEngComm*, 2013, **15**, 17.
111. D. A. Yang, H. Y. Cho, J. Kim, S. T. Yang and W. S. Ahn, *Energy Environ. Sci.*, 2012, **5**, 6465.
112. Z. Zhang, Z. Yao, S. Xiang and B. Chen, *Energy Environ. Sci.*, 2014, **7**, 2868.



PAF-1 and its derivatives contribute to the research on host-guest interaction and extends the application to wide fields.